

## EFFECT OF SONICATION ON THE PROPERTIES OF COMPOSITE POLYPYRROLE/MICROCELLULOSE AND ITS POTENTIAL AS A CAPACITOR

Berlian Sitorus<sup>1\*</sup>, Deni Pranata<sup>1</sup>, Mariana Bara'allo Malino<sup>2</sup>

<sup>1</sup>Department of Chemistry, FMIPA, Universitas Tanjungpura Pontianak, Jl. Prof. Dr. Hadari Nawawi, Pontianak, 78124, West Kalimantan, Indonesia

<sup>2</sup>Department of Physics, FMIPA, Universitas Tanjungpura Pontianak, Jl. Prof. Dr. Hadari Nawawi, Pontianak, 78124, West Kalimantan, Indonesia

\*Email: berlian.sitorus@chemistry.untan.ac.id

Received 27 September 2022

Accepted 24 November 2022

### Abstract

The research aims to see the effect of sonication on the properties and capacitance of composites made of microcellulose isolated from Oil Palm Empty Fruit Bunches and Polypyrrole (PPy). PPy is a conductive polymer limited by its inflexibility; hence PPy is blended with microcellulose which can serve as a good matrix to increase the flexibility of PPy. The procedure to isolate the microcellulose was done by delignification, bleaching, and hydrolysis. In order to see the effect of sonication, hydrolysis was undertaken in two different ways : (i) without sonication and (ii) using sonication. Besides, the polymerization time for pyrrole was also varied: 4 and 16 hours and simultaneously composited with each microcellulose from (i) and (ii). The results show an increase in cellulose crystallinity from 35.6% without sonication to 40% after sonication, while the diameter of the sonicated microcellulose fibers tends to be smaller than the counterpart. The 4-hour polymerization time shows that the composite containing the unsonicated microcellulose has a higher capacitance than the composite with the sonicated microcellulose, 14.8 nF and 8.8 nF, respectively. Meanwhile, a similar capacitance is measured for the 16-hour polymerization, 1.90 nF and 2.68 nF, using the sonicated and un-sonicated microcellulose. Overall, although the capacitances of the composites are in the nanofarad scale, it can be said that the composite can be potentially used as a capacitor.

**Keywords:** microcellulose, oil palm empty fruit bunches, polypyrrole, sonication

### Introduction

Fossil fuels are one of the largest energy sources that fulfill most aspects of life, including transportation, electricity supply needs, food, and industry. However, its nature as a non-renewable energy source means it will eventually run out. Therefore, countries in the world are currently competing with each other to create new renewable energy sources. Implementing new and renewable energy (NRE) is a solution that must be implemented to achieve the milestone of independence and national energy security (Pinilih & Chairunnisa, 2019)

One of the obstacles faced in the implementation of NRE is energy storage. For instance, the intensity of solar energy is unstable and has limited irradiation time, where the optimum irradiation intensity is during the day (about 5–6 hours). Likewise, the wind strength is unstable and varies depending on the airflow mass. Therefore, developing energy storage materials is very important in efforts to improve the implementation of NRE.

Polypyrrole (PPy) is one of the conductive polymers with an electrical conductivity of  $1.55 \text{ S cm}^{-1}$  (Y. Li *et al.*,



2017). It is easy to synthesize because it can be produced at room temperature. In addition, PPy has advantages such as high stability, high conductivity, and good redox properties compared to other types of conductive polymers, so it is often applied as batteries or supercapacitors. However, according to (Zhuo *et al.*, 2019), the main issue with using conductive polymers as capacitors is poor cycle stability due to changes in volume during the charge-discharge process (charge-discharge process). Various composites which combine the accumulation of electrostatic charges and redox reactions have been investigated to overcome the drawbacks of these conductive polymers. (Qian *et al.*, 2013) prepared graphene oxide (GO) or GO composites reduced with PPy, which can maintain 85% capacitance after 1000 cycles. However, the environmental hazard of synthesizing GO and the high cost and difficulty of manufacturing GO limit the large-scale application of the materials. Thus, biomass with large amounts of elemental carbon (C) is considered a sustainable carbon source and ideal for large-scale carbon production due to its low cost and renewable nature. As the most abundant and widely available biopolymer in nature, cellulose can be a sustainable carbon precursor for porous carbon, even serving as a desirable electrode for supercapacitors in the form of carbon aerogels (Zhang *et al.*, 2019). Besides, the rigidity of PPy as the other weakness can also be overcome by making PPy into a composite with a matrix as cellulose to produce a flexible and high conductivity composite (Deshmukh *et al.*, 2017). Cellulose can be used as a binder to manufacture flexible supercapacitor electrodes when composited with activated carbon as a capacitor (Murashko *et al.*, 2017).

Sonication is a method that utilizes sound energy from ultrasonic waves. The technique can overcome intermolecular

forces and disperse particles in solution to produce emulsions. The particles resulting from sonication can be micrometers in size to less than 100 nm. (Choudhury *et al.*, 2021) fabricated the reduced Fe<sub>3</sub>O<sub>4</sub>/graphene oxide nanocomposites and found that the composites produced through the sonication process showed better electrochemical performance than those made without sonication. Therefore, in this research, the fabrication of composite was applying the use of sonication.

The purpose of this study is to know the effect of the sonification process on the capacitance of capacitors made of PPy/microcellulose composite material from a natural resource. Cellulose can be obtained from the isolation and extraction process from lignocellulosic parts of the plants, such as Empty Fruit Bunch (EFB). It is known that the cellulose content in EFB is 45% (Adiguna *et al.*, 2020) which makes EFB a potential source of cellulose for use. Microcellulose was characterized using Fourier-Transform Infrared Spectroscopy (FTIR) to confirm the presence of cellulose and scanning electron microscope (SEM) to determine the surface morphology of the resulting microcellulose, along with its relationship to the resulting composite. The research novelty is the study of the sonication effect on PPy/microcellulose composites from EFB on the capacitance of the composite.

The cellulose was converted to microscale by further treating the isolated cellulose in two ways: (i) through sonication and (ii) without sonication. The PPy/microcellulose composite measured capacitance in a parallel plate capacitor was used to conclude the composite's potential as a capacitor.

## Research Methods

This section describes how PPy/microcellulose composites were fabricated and tested in terms of their capacitance. The process consisted of four

main stages: cellulose isolation from EFB, reduction of cellulose size into microcellulose, polymerization along with the formation of microcellulose-PPy composite, and making a parallel plate capacitor.

### Materials

Materials used in this research were hydrochloric acid (HCl), sulphuric acid (H<sub>2</sub>SO<sub>4</sub>), acetone (C<sub>2</sub>H<sub>6</sub>O), microcrystalline cellulose (C<sub>6</sub>H<sub>10</sub>O<sub>5</sub>)<sub>n</sub> sodium hydroxide (NaOH) (all from Merck, Germany). Pyrrole (C<sub>4</sub>H<sub>4</sub>NH) grade 98% from Sigma Aldrich, ethanol (C<sub>2</sub>H<sub>5</sub>OH), hydrogen peroxide (H<sub>2</sub>O<sub>2</sub>), and EFB from palm oil plants in West Kalimantan Province.

### Instrumentation

The equipment used in this study was an 80-mesh sieve, stirring rod, laboratory glassware, petri dish, Bucher funnula, desiccator, measuring cup, a condenser, a measuring flask, two neck flask, magnetic stirrer, analytical balance, an oscilloscope, oven, measuring pipette, grinder, spatula, and thermometer. Spectrophotometer Fourier Transform Infrared (FTIR) was used for functional groups. Scanning Electron Microscope (SEM) was used for morphological analysis, and X-Ray Diffractometer was used for crystallinity degree.

### Procedure

#### A. Production of PPy/microcellulose composites

EFB was washed and dried by drying in the sun and then mashed using a grinding machine. The refined EFB was then sieved using an-80 mesh sieve. EFB cellulose isolation refers to research conducted by (Aditama & Ardhyanta, 2017) and (William *et al.*, 2014) through 2 main stages: alkalization and bleaching. In the first stage, 8 grams of EFB was soaked with 2% NaOH (w/v) and stirred for 3 hours at 70°C. The solution was then filtered and tested for lignin existence by

reacting the filtrate with 72% (v/v) H<sub>2</sub>SO<sub>4</sub>.

The second stage was bleaching, where the residue was soaked in 1% NaOCl for 1 hour and 17.5% NaOH (w/v) for 30 minutes. Then, 7.2% H<sub>2</sub>O<sub>2</sub> was added to the residue and sonicated for 2 hours at 55°C. The solution was then filtered, and the residue was washed until neutral in pH. The isolated cellulose was then reduced in size by two methods: (i) without sonication and (ii) through sonication.

The procedure in method (i) was adapted from (Zhao *et al.*, 2018). Four grams of wet cellulose were added with 1.5 mol/L HCl solution with a ratio of cellulose and HCl solution of 2:20 and heated at 75 °C for 90 minutes using a magnetic stirrer. The mixture was then filtered, and the residue was washed using distilled water to a neutral pH, then centrifuged for 10 minutes at 3,000 rpm. The neutralized residue was then dried using the oven at 60 °C for 24 hours.

Method (i) process for producing microcellulose without going through sonication uses HCl for hydrolysis. When cellulose was dissolved in an HCl solution, the Cl<sup>-</sup> ions will weaken the β-glycosidic bonds to help the H<sup>+</sup> ions react with the glycosidic bonds between them will be broken, which will make the H bonds in the glycosidic structure open and produce glucose, then glucose undergoes protonation and produces hydronium ions (H<sub>3</sub>O<sup>+</sup>) (Trache *et al.*, 2016).

In method (ii), sonication was done by taking the cellulose from method (i) and dispersing it in 100 ml of distilled water. The suspension was sonicated for 1 hour at 40 kHz and 60 W, then centrifuged for 10 minutes at 3,000 rpm. The supernatant obtained was filtered, and the residue obtained was dried using an oven at 60°C for 24 hours. Sonication will cause a cavitation effect which changes the potential energy of the bubbles in the suspension into kinetic energy and results in collisions between the bubbles and the

cellulose surface. Relaxation will occur on the cellulose surface and cause the breaking of bonds between cellulose (Li *et al.*, 2012)

An amount of 0.3 g of microcellulose was composited with 3 ml of pyrrole. The mixture was stirred for 30 minutes using sonication, then added 0.25 ml of 0.1 M HCl solution and continued with the addition of 0.5 ml of FeCl<sub>3</sub>. The mixture was then sonicated for 30 minutes and then allowed to stand for 4 and 16 hours at room temperature for the polymerization process. After the polymerization was complete, the solution was filtered using a Buchner funnel, and the resulting composite was then washed with distilled water and ethanol. The composite was then dried in an oven at 60 °C for 24 hours and stored in a desiccator.

### B. Capacitance measurement

The measuring electrode plate consists of composite and graphite plates. The process was carried out by mixing 0.03 grams of polyvinyl acetate (PVA), dissolved in distilled water heated at 40 °C, with 0.3 grams of PPy/microcellulose composite (0.3 grams of graphite for graphite electrode plates) and stirred until thickened. The mixture was then attached to a 3 cm × 2.5 cm Aluminum plate, which previously was dipped in 1 M NaOH and dried. After tightening, the composite plate was dried at room temperature.

The composite and dry graphite plates were assembled asymmetrically, and a filter paper dripped with 1 M KOH solution was placed between the plates. The composite and graphite plates are then covered with parafilm to protect and attach the two electrode plates.

The results of the composite-cell plate and graphite have been formed asymmetrically to provide a higher voltage when compared to a symmetrical circuit (Magu *et al.*, 2019). Filter paper that has been added with KOH functions as a separator between the composite

electrode plate and graphite, while the KOH solution functions as an electrolyte in the cell plate circuit.

The capacitance of assembled cell plates was measured using Alternating Current (AC) electric current, with voltage variations of 2, 3, 4, 5, and 6 V. The given voltage was monitored through an oscilloscope, and the current was measured using an AC ampere meter. The current and voltage are then calculated based on Equations (1) and (2).

$$X_c = \frac{1}{2\pi fC} = \frac{V}{I} \quad (1)$$

$$C = \frac{1}{2\pi f} \cdot \frac{I}{V} \quad (2)$$

Where

$f = 50\text{Hz}$  is the frequency of

Alternating Current (AC),

$C$  = capacitance (Farad),

$V$  = voltage (Volt)

$I$  = current (A)

### Results and Discussion

In this section, the characteristics of the formed microcellulose are discussed first. There are two analyses applied to the microcellulose, i.e., FTIR and SEM. The characterization of microcellulose using FTIR aims to determine the functional groups of microcellulose produced. At this stage, the microcellulose spectra are compared with the pure microcellulose (Fareez *et al.*, 2018). Research results compared the wave numbers between the microcellulose produced and pure micro cellulose. While the SEM characterization is to determine the microcellulose diameter produced. Further, the capacitance value resulting from parallel plate capacitors will be discussed according to Equations (1) and (2).

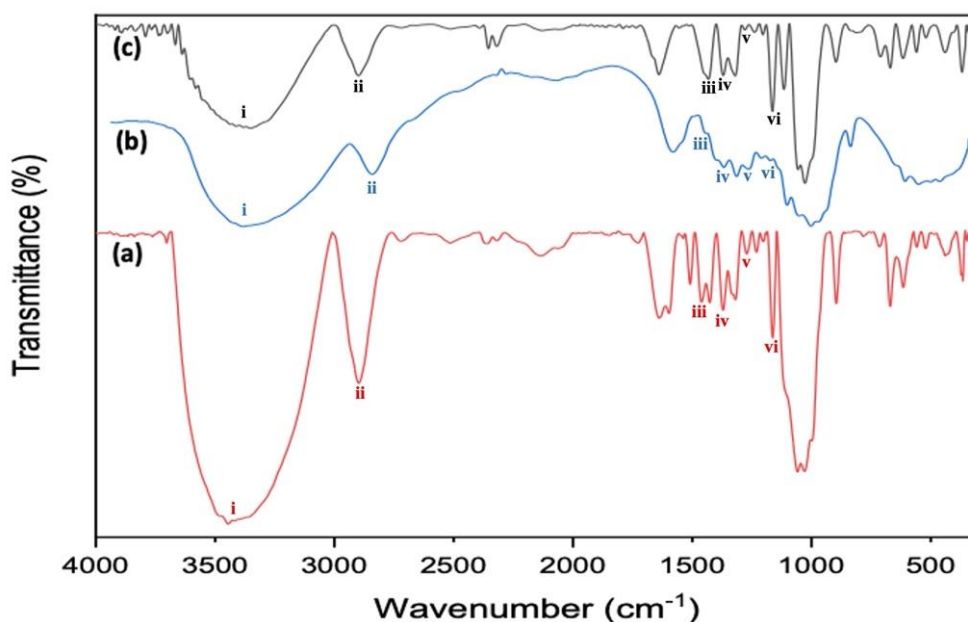
### FTIR Analysis

Table 1 shows the results of FTIR characterization of microcellulose that has been synthesized compared to pure

microcellulose based on the literature review results (Fareez et al., 2018). Figure 1 shows the FTIR spectra of the microcellulose obtained in the study.

**Table 1.** Comparison of microcellulose functional group identification and the wavenumber ( $\text{cm}^{-1}$ )

Functional Group/Peak label	Commercial Microcellulose	Microcellulose without sonication	Microcellulose with sonication	Microcellulose Fareez et al. (2018)
OH Stretching (i)	3352	3442	3444	3423
C-H Stretching asymmetric (ii)	2899	2900	2900	2897
C-O-H Bending (iii)	1334	1325	1332	1350
C-O-C Stretching (iv)	1163	1161	1163	1165
CH <sub>2</sub> Bending (vi)	1462	1452	1450	1460
C-C-H Bending (vi)	1275	1269	1278	1270



**Figure 1.** FTIR spectra of (a) commercial microcellulose, (b) microcellulose without sonication, and (c) microcellulose with sonication

From Table 1 and Figure 1, it can be seen that the microcellulose obtained has peaks that correspond to the theoretical microcellulose wave numbers. A broad absorption band seen at  $3400\text{--}3500\text{ cm}^{-1}$  or  $3000\text{--}3600\text{ cm}^{-1}$  in the spectra indicates -OH stretching vibrations of cellulose (Haafiz et al., 2013).

The absorption peaks of pure microcellulose and the study's results

(with and without sonication) at about  $3422$  and  $3444\text{ cm}^{-1}$  indicated the presence of hydrogen bonds from the O-H group, which is similar to the peak in (Fareez et al., 2018). Peaks at  $2899\text{--}2900\text{ cm}^{-1}$  indicated the presence of the C-H functional group, while the absorption peaks of  $1161\text{--}1165\text{ cm}^{-1}$  indicated the presence of the C-O-C group on  $\beta$ -glycosidic bonds (Hamdan et al., 2019).

Peaks at the wavenumber region of 1450–1462  $\text{cm}^{-1}$  indicated the presence of  $\text{CH}_2$  bending due to intermolecular hydrogen bonding at C6 of the aromatic ring group. At C6 of the aromatic ring group, C-H vibrations of cellulose associated with  $\beta$ -glycosidic bonds appear at 895–901  $\text{cm}^{-1}$ . So, it can be concluded that the isolation process of microcellulose has been successfully carried out.

### SEM analysis

SEM was used for the morphology and size analysis of the microcellulose, without sonication and using sonication with an image magnification of 2000 times, and then compared with commercial microcellulose. Based on the

SEM image and data analysis with ImageJ software, as shown in Figure 2 (b), sonicated microcellulose has a fiber length of 30  $\mu\text{m}$  and a diameter of about 5–7  $\mu\text{m}$ , while microcellulose without sonication (Figure 2 (c)) has a fiber length of 20  $\mu\text{m}$  and diameter in the range of 4–11  $\mu\text{m}$ . The commercial microcellulose has a fiber length of 20  $\mu\text{m}$  and a diameter of 3–7  $\mu\text{m}$ , the microcellulose produced from this research is still larger but has obtained micro size. The difference in the size of cellulose is caused by the condition of the aggregate in cellulose during the acid hydrolysis process, resulting in different sizes.

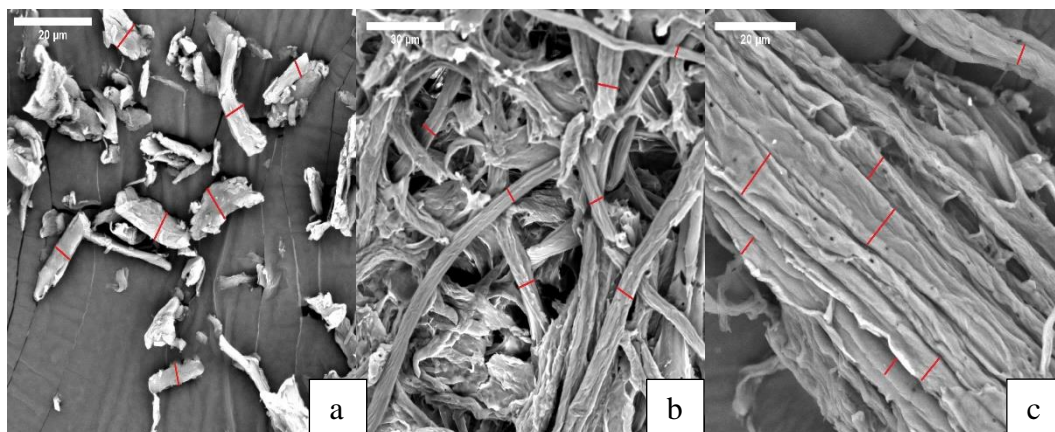


**Figure 2.** SEM images of (a) commercial microcellulose, (b) microcellulose with sonication, and (c) microcellulose without sonication. The red line indicates the measured fiber diameter.

Based on the SEM image in Figure 2 (b) and (c), it can be observed that the microcellulose produced in this study has the shape of long fibers (microfiber). The change in cellulose size from EFB to micro size because the cellulose hydrolysis process has made the amorphous areas of cellulose dissolve in acid and cut the  $\beta$ -1-4 bonds in the long chain of cellulose form cellulose fibers with smaller sizes (Supian *et al.*, 2018). Cellulose with sonication has a smaller average fiber diameter of 5.69  $\mu\text{m}$  or about 11% smaller than the average fiber

diameter of microcellulose without sonication.

### Polymerization

The isolated microcellulose was used to make PPy/microcellulose composites by an oxidative method. Pyrrole is added to microcellulose with the help of sonication to disperse the pyrrole solution on microcellulose so that the polymerization process on microcellulose becomes evenly distributed (Srivastava *et al.*, 2020).  $\text{FeCl}_3$  is an oxidator that will make the pyrrole monomers into radical active cations, thus forming a bond

between two monomers at the  $\alpha$ -carbon position. Dihydroneer cations formed will then release 2 protons and form dimers. This process will continue to create long PPy, while the  $\text{FeCl}_3$  will create  $\text{FeCl}_2$  and  $\text{HCl}$  in the suspension solution after the polymerization reaction occurs. PPy polymerization will stop when there is no  $\text{FeCl}_3$  in the suspension. If the concentration of  $\text{FeCl}_3$  is smaller than the amount of polymerized pyrrole, it produces imperfect PPy with short conjugate bonds (Chen *et al.*, 2019; Gahlout & Choudhary, 2016).

The PPy chain that has been formed was then doped using  $\text{HCl}$  as a dopant during the polymerization process. The reduced electron density value on the PPy carbon atom causes it to oxidize and produce a positive charge on the PPy polymer. The negative charge of the dopant will be bound to the carbon atoms of the PPy backbone due to ionic interactions. PPy/microcellulose

composites are formed when the imine group of the PPy chain and the hydroxyl bond in microcellulose form hydrogen bonds to form aggregates in microcellulose.

#### XRD analysis

XRD analysis was performed mainly to determine the degree of crystallinity and the crystal type of microcellulose. Based on the resulting diffractogram, as shown in Figure 3, the commercial microcellulose crystalline diffraction pattern has  $2\theta = 15.6^\circ$ ,  $22.5^\circ$ , and  $34.3^\circ$ . In the isolated cellulose from EFB, the diffraction pattern of the crystalline microcellulose with sonication peaked at  $2\theta = 12.1^\circ$ ,  $22^\circ$ , and  $35^\circ$ , while the counterpart shows peaks at  $2\theta = 14.5^\circ$ ,  $22.7^\circ$ , and  $35.5^\circ$ . According to (Daicho *et al.*, 2018), microcellulose has three characteristic peaks related to the crystalline area in microcellulose ( $2\theta = 22^\circ$ ,  $35^\circ$ , and  $14^\circ$ ).

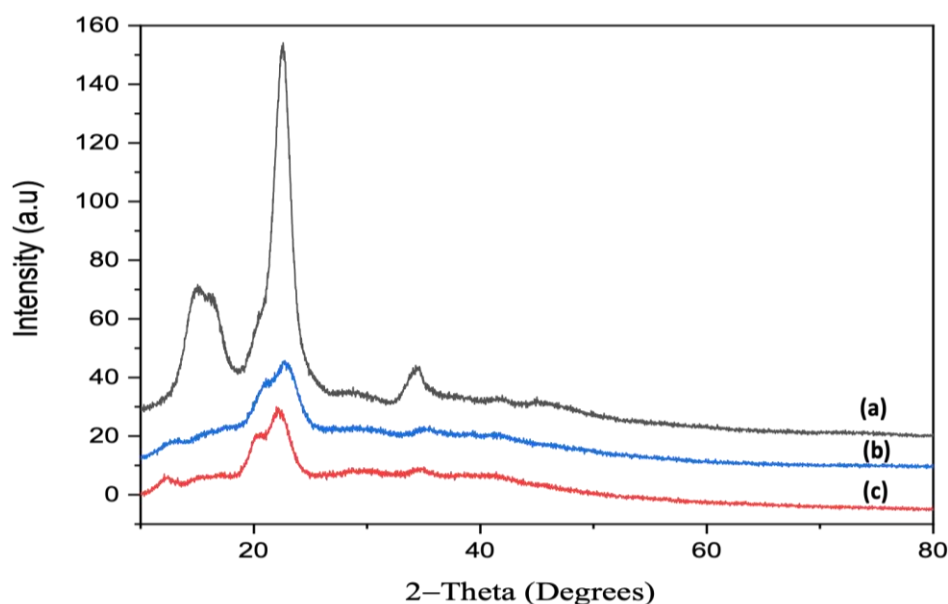


**Figure 3.** X-Ray Diffractogram of (a) commercial microcellulose, (b) microcellulose without sonication, and (c) microcellulose with sonication.

The sonication process is carried out to help disperse and prevent the agglomeration of cellulose (Pereira *et al.*, 2020). Ultrasonic waves will cause cavitation, where the effect of this

radiation forms gas bubbles that move at high speeds so that mechanical energy is formed, which can disrupt the hydrogen bond network in cellulose. This energy, in large quantities, can diffuse dissociated

H<sup>+</sup> ions from acid into the cellulose framework and damage the amorphous

portion of the cellulose (Hamid *et al.*, 2016; Holilah *et al.*, 2022).

**Table 2.** Crystallinity degree of microcelluloses

	<b>Commercial microcellulose</b>	<b>Microcellulose without sonication</b>	<b>Microcellulose with sonication</b>
Crystallinity degree	81 %	35.60 %	40 %

#### Capacitance Test

The PPy/microcellulose composite is then used as a capacitor electrode, where the composite is superimposed on an aluminum plate that acts as a current collector. The capacitance of the organic

capacitor based on the micro cellulose/PPy composite with variations in microcellulose production through sonication and without sonication is depicted in Table 3.

**Table 3.** The capacitance of PPy/microcellulose composite from 4 and 16 hours of polymerization

<b>The capacitance of the composite consists of microcellulose (nF)</b>				
Voltage (Volt)	Without sonication		With sonication	
	4 hours	16 hours	4 hours	16 hours
2	11.6	2.39	7.2	1.79
3	14	2.62	8.3	2.10
4	15.4	2.87	9.3	1.91
5	16.2	2.65	9.7	1.47
6	16.6	2.87	9.9	2.23
<b>Average</b>	<b>14.8</b>	<b>2.68</b>	<b>8.9</b>	<b>1.90</b>

Table 3 shows that the capacitance of the capacitor with PPy/microcellulose composite without the sonication process has a slightly higher capacitance value than the sonicated PPy/microcellulose composite. This is because the cavitation process generated from ultrasonic waves during the sonication process assists in making smaller agglomerates that occur due to the exposure of the waves to the composite material. The shock waves of sonication can separate agglomeration resulting in smaller particle size and reducing porosity in the cellulose. This is because the porosity of the composite is reduced so that the ion transfer becomes slow and changes the resulting capacitance; the drying process of the

composite can cause reduced porosity. The pores in the composite significantly affect the resulting conductivity because it helps accelerate the rate of anion transfer throughout all areas of the composite (Carlsson *et al.*, 2012).

Although the resulting capacitor has a relatively small capacitance (on the nano order), it must be noted that the capacity of the parallel plate capacitor depends not only on the filler material but also on the surface area of the capacitor and the distance between the two plates. In this study, the capacitor size used is 3 × 2.5 cm with a distance of 1 cm between the plates. Thus, the resulting capacitance value is relatively small.



## Conclusions

In this study, an idea was initiated to manufacture PPy/microcellulose composites from EFB and discern the capacitance of composites as capacitors by using them as a substance in parallel plate capacitors. Characterization of the isolated cellulose shows it can be concluded that sonicated microcellulose tends to have an 11% smaller diameter from the microcellulose than the unsonicated microcellulose. The composite consisting of unsonicated microcellulose in 4 hours has a higher capacitance than the sonicated microcellulose, while the longer polymerization time, 16 hours, results in similar capacitance of both composite variations. Although the resulting capacitance is in the nanofarad scale, it can be said that the PPy/microcellulose composites produced have the potential to be used as capacitors.

## Acknowledgment

The authors are highly thankful to the Fakultas MIPA in Universitas Tanjungpura for financial support for this research (Hibah DIPA-Year 2021).

## Conflict of Interest

The authors have no conflict of interest.

## Author Contributions

DP conducted the experiment, MBM conducted the calculations on crystallinity degree from XRD, BS and DP wrote and revised the manuscript. All authors agreed to the final version of this manuscript.

## References

Adiguna, G. S., Nyoman, I. and Aryantha, P., 2020. Aplikasi fungi rizosfer sebagai pupuk hayati pada bibit kelapa sawit dengan memanfaatkan limbah tandan kosong kelapa sawit sebagai media pertumbuhan. *Manfish*, 1(1).

Aditama, A. G. and Ardhyana, H., 2017. Isolasi Selulosa dari Serat Tandan Kosong Kelapa Sawit untuk Nano Filler Komposit Absorpsi Suara: Analisis FTIR. *Jurnal Teknik ITS*, 6(2), F229–F232.

Carlsson, D. O., Nyström, G., Zhou, Q., Berglund, L. A., Nyholm, L. and Stromme, M., 2012. Electroactive nanofibrillated cellulose aerogel composites with tunable structural and electrochemical properties. *Journal of Materials Chemistry*, 22(36), 19014–19024.

Chen, Y., Wang, F., Dong, L., Li, Z., Chen, L., He, X., Gong, J., Zhang, J. and Li, Q., 2019. Design and optimization of flexible polypyrrole/bacterial cellulose conductive nanocomposites using response surface methodology. *Polymers*, 11(6), 960.

Choudhury, B. J., Roy, K. and Moholkar, V. S., 2021. Improvement of Supercapacitor Performance through Enhanced Interfacial Interactions Induced by Sonication. *Industrial and Engineering Chemistry Research*, 60(20).

Daicho, K., Saito, T., Fujisawa, S. and Isogai, A., 2018. The Crystallinity of Nanocellulose: Dispersion-Induced Disordering of the Grain Boundary in Biologically Structured Cellulose. *ACS Applied Nano Materials*, 1(10), 3934–3942.

Deshmukh, K., Basheer Ahamed, M., Deshmukh, R. R., Khadheer Pasha, S. K., Bhagat, P. R. and Chidambaram, K., 2017. Biopolymer Composites with High Dielectric Performance: Interface Engineering. In *Biopolymer Composites in Electronics*.

Fareez, I. M., Ibrahim, N. A., Wan Yaacob, W. M. H., Mamat Razali, N. A., Jasni, A. H. and Abdul Aziz, F., 2018. Characteristics of cellulose extracted from Jospine pineapple leaf fibre after alkali treatment

- followed by extensive bleaching. *Cellulose*, 25(8).
- Gahlout, P. and Choudhary, V., 2016. Tailoring of polypyrrole backbone by optimizing synthesis parameters for efficient EMI shielding properties in X-band (8.2–12.4 GHz). *Synthetic Metals*, 222, 170–179.
- Haafiz, M. K. M., Hassan, A., Zakaria, Z., Inuwa, I. M., Islam, M. S. and Jawaid, M., 2013. Properties of polylactic acid composites reinforced with oil palm biomass microcrystalline cellulose. *Carbohydrate Polymers*, 98(1).
- Hamdan, M. A., Ramli, N. A., Othman, N. A., Mohd Amin, K. N. and Adam, F., 2019. Characterization and property investigation of microcrystalline cellulose (MCC) and carboxymethyl cellulose (CMC) filler on the carrageenan-based biocomposite film. *Materials Today: Proceedings*, 42, 56–62.
- Hamid, S. B. A., Zain, S. K., Das, R. and Centi, G., 2016. Synergic effect of tungstophosphoric acid and sonication for rapid synthesis of crystalline nanocellulose. *Carbohydrate Polymers*, 138, 349–355.
- Holilah, H., Bahruji, H., Ediati, R., Asranudin, A., Jalil, A. A., Piluharto, B., Nugraha, R. E. and Prasetyoko, D. (2022). Uniform rod and spherical nanocrystalline celluloses from hydrolysis of industrial pepper waste (*Piper nigrum* L.) using organic acid and inorganic acid. *International Journal of Biological Macromolecules*, 204, 593–605. <https://doi.org/10.1016/j.ijbiomac.2022.02.045>
- Li, W., Yue, J. and Liu, S., 2012. Preparation of nanocrystalline cellulose via ultrasound and its reinforcement capability for poly(vinyl alcohol) composites. *Ultrasonics Sonochemistry*, 19(3), 479–485.
- Li, Y., Bober, P., Trchová, M. and Stejskal, J., 2017. Polypyrrole prepared in the presence of methyl orange and ethyl orange: Nanotubes versus globules in conductivity enhancement. *Journal of Materials Chemistry C*, 5(17), 4236–4245.
- Magu, T., Augustine, A., Louis, H. and Peter, D., 2019. A Review on Conducting Polymers-Based Composites for Energy Storage Application. *Journal of Chemical Reviews*, 1(1), 19–34.
- Murashko, K., Nevstrueva, D., Pihlajamäki, A., Koiranen, T. and Pyrhönen, J., 2017. Cellulose and activated carbon based flexible electrical double-layer capacitor electrode: Preparation and characterization. *Energy*, 119, 435–441.
- Pereira, P. H. F., Ornaghi Júnior, H. L., Coutinho, L. V., Duchemin, B. and Cioffi, M. O. H., 2020. Obtaining cellulose nanocrystals from pineapple crown fibers by free-chlorite hydrolysis with sulfuric acid: physical, chemical and structural characterization. *Cellulose*, 27(10), 5745–5756.
- Pinilih, S. A. G. and Chairunnisa, W. L., 2019. New and Renewable Energy Policy in Developing Indonesia's National Energy Resilience. *E3S Web of Conferences*, 125.
- Qian, T., Yu, C., Wu, S. and Shen, J., 2013. A facile prepared polypyrrole-reduced graphene oxide composite with a crumpled surface for high performance supercapacitor electrodes. *Journal of Materials Chemistry A*, 1(22), 6539–6542.
- Srivastava, V. K., Jain, P. K., Kumar, P., Pegoretti, A. and Bowen, C. R., 2020. Smart Manufacturing Process of Carbon-Based Low-Dimensional Structures and Fiber-Reinforced Polymer Composites for Engineering Applications. In *Journal of Materials*

- Engineering and Performance* (Vol. 29, Issue 7, pp. 4162–4186).
- Supian, M. A. F., Mohd Amin, K. N., Jamari, S. S. and Mohamad, S., 2018. Investigation On Pre-Treatment Process In Microcrystalline Cellulose (Mcc) From Oil Palm Empty Fruit Bunch (Efb). *Journal Of Chemical Engineering And Industrial Biotechnology*, 3(1), 87–96.
- Trache, D., Hussin, M. H., Hui Chuin, C. T., Sabar, S., Fazita, M. R. N., Taiwo, O. F. A., Hassan, T. M. and Haafiz, M. K. M., 2016. Microcrystalline cellulose: Isolation, characterization and bio-composites application—A review. In *International Journal of Biological Macromolecules* (Vol. 93, pp. 789–804).
- William, R. A., Sitorus, B. and Malino, M. B., 2014. Sintesis Polianilin Pada Matriks Selulosa Sebagai Elektrolit Padat Pada Model Baterai Sederhana. *Jkk*, 3(4).
- Zhang, X., Li, H., Zhang, W., Huang, Z., Tsui, C. P., Lu, C., He, C. and Yang, Y., 2019. In-situ growth of polypyrrole onto bamboo cellulose-derived compressible carbon aerogels for high performance supercapacitors. *Electrochimica Acta*, 301, 55–62.
- Zhao, T., Chen, Z., Lin, X., Ren, Z., Li, B. and Zhang, Y., 2018. Preparation and characterization of microcrystalline cellulose (MCC) from tea waste. *Carbohydrate Polymers*, 184, 164–170.
- Zhuo, H., Hu, Y., Chen, Z. and Zhong, L., 2019. Cellulose carbon aerogel/PPy composites for high-performance supercapacitor. *Carbohydrate Polymers*, 215, 322–329.